Science of the Total Environment 603–604 (2017) 406–415

Contents lists available at ScienceDirect

Science of the Total Environment

journal homepage: www.elsevier.com/locate/scitotenv

Unraveling the complexities of the velocity dependency of *E. coli* retention and release parameters in saturated porous media

Salini Sasidharan [a,b,c,d,f,*], Scott A. Bradford [d], Saeed Torkzaban [c], Xueyan Ye [e], Joanne Vanderzalm [a], Xinqiang Du [e], Declan Page [a]

[a] CSIRO, Land and Water, Glen Osmond, SA 5064, Australia
[b] National Centre for Groundwater Research and Training, Adelaide, SA 5001, Australia
[c] Flinders University, Adelaide, SA 5001, Australia
[d] USDA, ARS, Salinity Laboratory, Riverside, CA 92507, United States
[e] Key Laboratory of Groundwater Resources and Environment, Ministry of Education, Jilin University, Changchun 130021, China
[f] Department of Environmental Sciences, University of California, Riverside, California, United States

HIGHLIGHTS

- The velocity dependency of cell retention and release parameters were investigated under different IS conditions.
- The sticking efficiency, retention capacity, and irreversible cell retention increased with ionic strength and decreasing water velocity.
- The probability for cells to diffuse over the energy barrier depends on the residence time on heterogeneous surfaces.
- The adhesive strength increased with the residence time and decreasing water velocity.
- Torque balance consideration explained the negligible cell removal with large increases in velocity, and large amounts of cell release following sand excavation.

GRAPHICAL ABSTRACT

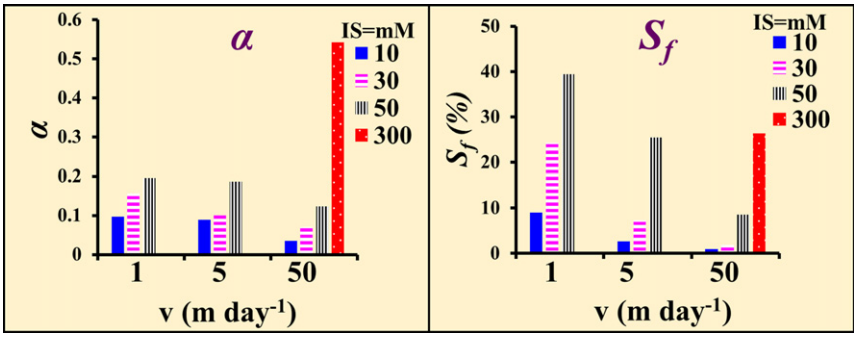

ARTICLE INFO

Article history:
Received 28 April 2017
Received in revised form 10 June 2017
Accepted 11 June 2017
Available online 19 June 2017

Editor: D. Barcelo

Keywords:
Bacteria
Flow velocity
Residence time
Sticking efficiency

ABSTRACT

Escherichia coli transport and release experiments were conducted to investigate the pore-water velocity (v) dependency of the sticking efficiency (α), the fraction of the solid surface area that contributed to retention (S_f), the percentage of injected cells that were irreversibly retained (M_{irr}), and cell release under different (10–300 mM) ionic strength (IS) conditions. Values of α, S_f, and M_{irr} increased with increasing IS and decreasing v, but the dependency on v was greatest at intermediate IS (30 and 50 mM). Following the retention phase, successive increases in v up to 100 or 150 m day^{-1} and flow interruption of 24 h produced negligible amounts of cell release. However, excavation of the sand from the columns in excess electrolyte solution resulted in the release of >80% of the retained bacteria. These observations were explained by: (i) extended interaction energy calculations on a heterogeneous sand collector; (ii) an increase in adhesive strength with the residence time; and (iii) torque balance consideration on rough surfaces. In particular, α, S_f, and M_{irr} increased with IS due to lower energy barriers and stronger primary minima. The values of α, S_f, and M_{irr} also increased with decreasing v because the

Abbreviations: IS, ionic strength; BTC, breakthrough curves.

* Corresponding author at: USDA, ARS, Salinity Laboratory, Riverside, CA 92507, United States.
E-mail address: salinis@ucr.edu (S. Sasidharan).

http://dx.doi.org/10.1016/j.scitotenv.2017.06.091

Retention
Surface roughness

adhesive strength increased with the residence time (e.g., an increased probability to diffuse over the energy barrier) and lower hydrodynamic forces diminished cell removal. The controlling influence of lever arms at microscopic roughness locations and grain-grain contacts were used to explain negligible cell removal with large increases in v and large amounts of cell recovery following sand excavation. Results reveal the underlying causes (interaction energy, torque balance, and residence time) of the velocity dependency of *E. coli* retention and release parameters (k_{sw}, α, and S_f) that are not accounted for in colloid filtration theory.

1. Introduction

An improved understanding of processes that control the transport, retention, and release of bacteria in porous media is needed for many environmental and industrial applications such as bioremediation of contaminated soils and aquifers, and filtration of pathogenic microorganisms in groundwater or engineered water treatment systems (Liu et al., 2007; Redman et al., 2004). A number of physical, chemical, and biological factors control the retention of bacteria in porous media, including: soil texture (Morales et al., 2015), temperature (McCaulou et al., 1995; Morales et al., 2015), water velocity (Hendry et al., 1999; Meinders et al., 1995), bacterial surface properties (Bolster et al., 2000; Liu et al., 2007; Vandevivere and Baveye, 1992), bacterial motility (de Kerchove and Elimelech, 2008; Huysman and Verstraete, 1993; Massoudieh et al., 2013), solution chemistry (Gannon et al., 1991; Massoudieh et al., 2013; Redman et al., 2004; Simoni et al., 2000; Tong et al., 2005), solid surface roughness (Shellenberger and Logan, 2002), and chemical heterogeneities (Schulze-Makuch et al., 2003; Yee et al., 2000). Although the influence of water velocity on bacteria retention has been studied for many years (Hendry et al., 1999; Meinders et al., 1995), there still are important gaps in knowledge.

Colloid filtration theory (Tufenkji and Elimelech, 2004a; Yao et al., 1971) has been commonly used to explain the transport and retention of bacteria in porous media under saturated conditions. According to colloid filtration theory, the retention rate coefficient (k_{sw}) is a function of the single-collector efficiency (η), the sticking efficiency (α), and the pore-water velocity (v). In particular, k_{sw} is dependent on the mass transfer of colloids from the bulk solution to the collector (sand grain) surface via Brownian diffusion, interception, and sedimentation which is quantified by η (Schijven and Hassanizadeh, 2000; Tufenkji and Elimelech, 2005). Correlation equations have been established from pore-scale simulations of colloid transport to predict η as a function of water velocity, diffusion coefficient, colloid size and density, and collector (grain) diameter and porosity (Ma et al., 2013; Messina et al., 2015; Nelson and Ginn, 2011; Rajagopalan and Tien, 1976; Tufenkji and Elimelech, 2004a; Yao et al., 1971). Colloid filtration theory predicts that differences in the rates of colloid mass transfer cause a nonlinear increase in k_{sw} with v for a given value of α (Tufenkji and Elimelech, 2004b). The fraction of colloid collisions with the collector surface that produces retention (e.g., immobilization) is quantified by the parameter α which changes with the solution and solid phase chemistries (Schijven and Hassanizadeh, 2000; Tufenkji and Elimelech, 2004a). Colloid filtration theory assumed that α only depends on the irreversible adhesive interaction between the colloid and collector surface, but was independent of the water velocity (Elimelech et al., 1998; Elimelech and O'Melia, 1990). In contrast, measured and theoretical values of α and the maximum concentration of colloids on the solid phase (S_{max}) have been shown to depend on solution chemistry and water velocity (Bradford et al., 2012; Johnson et al., 2007; Li and Johnson, 2005; Sasidharan et al., 2014; Shen et al., 2010; Tong et al., 2005; Torkzaban et al., 2007). The value of S_{max} is proportional to the fraction of the solid surface area that contributed to the retention (S_f) (Bradford et al., 2011a; Bradford et al., 2011b; Kim et al., 2009a; Sasidharan et al., 2014). In addition, only a fraction of immobilized colloids is irreversibly retained (Torkzaban and Bradford, 2016; Torkzaban et al., 2010). However, the coupled role of solution chemistry and water velocity on α, S_f, and the reversibility of colloid retention have not yet been completely studied and explained.

Bacteria retention and release depend on the balance of forces and/or torques that act on cells adjacent to the solid-water interface (Bergendahl and Grasso, 2000; Bradford et al., 2009; Bradford et al., 2011b; Li et al., 2005; Torkzaban et al., 2007; Torkzaban et al., 2008). For neutrally buoyant bacteria, these forces and/or torques arise from adhesive interactions, random Brownian diffusion, and system hydrodynamics (Ahmadi et al., 2007; Bergendahl and Grasso, 2000; Bradford et al., 2009; Cushing and Lawler, 1998; Goldman et al., 1967; Johnson et al., 1971; O'Neill, 1968; Sharma et al., 1992; Soltani and Ahmadi, 1994; Torkzaban et al., 2007; Torkzaban et al., 2008). Consequently, colloid filtration theory assumes that adhesive interactions always dominant over Brownian diffusion and hydrodynamic forces and torques. In reality, the strength of the adhesive force and torque depends on the solution and solid phase chemistries, colloid size and shape, nanoscale roughness and chemical heterogeneity, deformation, and grain topography (Bayoudh et al., 2009; Bolster et al., 2001; Bradford and Torkzaban, 2012; Bradford and Torkzaban, 2013; Bradford and Torkzaban, 2015; Bradford et al., 2011b; Elimelech, 1994; Kim et al., 2009b; Shen et al., 2013; Shen et al., 2012; Suresh and Walz, 1996; Torkzaban and Bradford, 2016; Torkzaban et al., 2007; Torkzaban et al., 2008; Walker et al., 2005). The hydrodynamic force and torque depend on the average pore-water velocity, the grain size distribution, microscopic roughness, porosity, and colloid size (Bradford et al., 2011b; Burdick et al., 2001; Kuznar and Elimelech, 2007; O'Neill, 1968; Saffman, 2006; Torkzaban et al., 2007; Torkzaban et al., 2008). In many instances, the strength of the adhesive interaction is weak, and a fraction of retained colloids are susceptible to diffusive and/or hydrodynamic removal (Torkzaban et al., 2007; Wang et al., 2016). This result has been used to explain the velocity dependency of α and S_f (Torkzaban et al., 2007).

Not all factors that influence adhesive and hydrodynamic forces and torques have been considered in previous studies that examined the velocity dependency of α and S_f. For example, some researchers have also reported that the adhesive interaction increases with the residence time (Hemmerle et al., 1999; Meinders et al., 1994; Meinders et al., 1995; Mondon et al., 2003; Stuart and Hlady, 1995; Torkzaban et al., 2013; Vadillo-Rodriguez et al., 2004; Xu and Logan, 2006; Xu et al., 2005). This finding has typically been related to the formation of chemical bonds (Vadillo-Rodriguez et al., 2004; Xu and Logan, 2006), but may also be explained by an increase in the probability that random Brownian motion will produce a kinetic energy of sufficient strength to overcome an energy barrier to achieve a deeper minimum in the interaction energy (Bradford and Torkzaban, 2015; Sasidharan et al., 2017; Torkzaban and Bradford, 2016). An increase in the adhesive interaction with the residence time has important implications for the velocity dependency of α and S_f that have not yet been explained. In particular, the residence time is inversely related to the advective transport velocity. This implies that lower water velocities and flow interruptions with larger residence times may produce greater bacteria retention and less release because of the greater adhesive strength. Furthermore, initially weakly associated colloids that are temporally immobilized in low velocity regions, microscopic roughness locations, and/or grain-grain contacts can experience less diffusive and/or hydrodynamic release with increasing residence time because of an increase

in the adhesive interaction. Consequently, temporal immobilization at such locations may be an importance precursor to more permanent colloid retention.

The primary objective of this study was to experimentally and theoretically investigate the causes (e.g., interaction energy on heterogeneous surface, residence time, and torque balance) of the velocity dependency of retention and release parameters (k_{sw}, α, S_{max}, and S_f) for *Escherichia coli* in saturated porous media. The transport and retention of *E. coli* was systematically studied under various ionic strength (IS) and water velocity conditions. Values of k_{sw} and S_{max} were then obtained by fitting to observed breakthrough curves (BTCs), and the velocity dependency of calculated α and S_f was determined. Cell release was then investigated with step increases in the water velocity, a 24-h flow interruption, and following excavation of the sand into an excess volume of the electrolyte solution of the same solution chemistry. Additionally, the interaction energy between a chemically and physically heterogeneous collector (sand grain) and a homogeneous colloid (bacteria) was calculated. Results from this work improve our understanding of the roles of residence time and nanoscale and microscopic roughness in determining the dependency of α and S_f on velocity and solution chemistry.

2. Materials and method

2.1. Porous media and electrolyte solutions

Natural graded river sand (River sand Pty Ltd.) with a particle size distribution between 125 and 300 μm was employed in column transport experiments. This sand was cleaned using an acid washing and boiling procedure described by Sasidharan et al. (2014). Electrolyte solutions of 10, 30, 50, and 300 mM were prepared using analytical grade NaCl and Milli-Q water at unadjusted pH = 5.5–5.8 as in many previous studies (Walker et al., 2004; Zhang et al., 2010).

2.2. Bacteria preparation

A non-pathogenic strain of *Escherichia coli* ATCC 13706 was employed in transport studies. The bacteria were prepared by growing overnight, pelleting, and washing using a procedure explained in Sasidharan et al. (2017). The bacterial pellet was then diluted into the desired electrolyte solution to achieve a final absorbance of 0.45 at a wavelength of 460 nm, which corresponds to an initial bacterial influent concentration (C_0) of ~10^8 cells mL^{-1}. Samples from column experiments were analyzed by measuring the absorbance at 460 nm by UV–vis spectrophotometry (SpectraMax Plus 384, US).

2.3. Zeta potential and size measurements

The electrophoretic mobilities of bacteria and crushed sand (<2 μm) suspended in electrolyte solutions were measured at room temperature using a Zetasizer (Malvern, Zetasizer Nano Series, Nano-ZS). The Smoluchowski equation (Elimelech et al., 1994) was used to convert the measured electrophoretic mobilities values to zeta potentials. Dynamic light scattering (DLS) in the Zetasizer was used to determine hydrodynamic radii of these bacteria suspensions. (Malvern Instruments Ltd., 2004).

2.4. Column preparation and transport experiments

Column experiments were conducted in sterilized polycarbonate columns (11 cm height and 1.9 cm internal diameter). The columns were wet packed using clean sand while vibrating the column to liberate entrapped air. After packing, the columns were preconditioned with >6 pore volumes of a selected electrolyte solution using a syringe pump (Model 22, Harvard Apparatus) at a pore-water velocity (v) of 5 m day^1.

The bacteria suspension at selected IS (10, 30, 50, and 300 mM Na^+) was introduced into the column using a syringe pump at an average v of 1, 5, and 50 m day^{-1} (Darcy velocity of 0.4, 2, and 20 m day^{-1}, respectively) for 10 pore volumes (Phase I). The corresponding residence time is equal to 158.4, 31.7, and 3.2 min when $v = 1$, 5, and 50 m day^{-1}, respectively. This phase was followed by injection of several pore volumes of bacteria-free-electrolyte solution at the same IS and pore water velocity (Phase II). The release of retained bacteria was investigated during Phase III by step increases of v from 10 to 150 m day^{-1} (depending on the hydrodynamic conditions during Phases I and II). The effect of residence time on bacteria release was further investigated by employing a 24 h flow interruption and resuming the flow at v = 5 m day^{-1} (Phase IV). The column effluent samples were collected using a Spectra/Chrom® CF-1 Fraction Collector and the concentration of bacteria was quantified using the method explained in Section 2.2. The reproducibility of column experiments was verified by conducting replicates under selected experimental conditions.

Following the completion of bacteria retention and release phases (Phase I to IV), the column was dissected in 1 cm segments (11 layers) during Phase V. The sand from each segment was placed in a vial containing 20 mL of the same electrolyte solution used in Phase I. The vials were shaken on a tube rotator for 30 min and the recovered bacteria concentration was measured using the method explained in Section 2.2. The sand was dried and the water and sand mass in each segment were determined. Some of the collected sand grains were examined using a scanning electron microscope (SEM Quanta 450, Adelaide Microscopy) for roughness features and irreversibly retained bacteria.

A mass balance was conducted for the bacteria in the column experiments using information on injected and recovered cells during Phases I–V. The percentage of injected cells that was recovered during Phases I, II, III, IV, and V was denoted as M_{I}, M_{II}, M_{III}, M_{IV}, and M_{V}, respectively. The percentage of bacteria mass retained on the solid phase (M_s) was determined as the difference in the mass of injected cells and mass of cells recovered in the effluent breakthrough curve ($M_{BTC} = M_{\mathrm{I}} + M_{\mathrm{II}}$) during Phases I and II. The percentage of injected cells that were irreversibly retained (M_{irr}) was determined as 100-M_{BTC}-M_{III}-M_{IV}-M_{V}.

3. Theoretical analysis

3.1. BTC simulations

The experimental BTCs for bacteria were simulated using the HYDRUS-1D model (Simunek JvG and Sejna, 2005). The HYDRUS-1D program numerically solves the Richards' equation for variably saturated water flow and Fickian-based advection-dispersion equations for heat and solute transport. The governing continuum-scale flow and transport equations are solved numerically using Galerkin-type linear finite element schemes (Simunek JvG and Sejna, 2005). The following aqueous and solid phase mass balance equations were considered in this model.

$$\frac{\partial C}{\partial t} = \lambda v \frac{\partial^2 C}{\partial z^2} - v \frac{\partial C}{\partial z} - r_{sw} \tag{1}$$

$$r_{sw} = \frac{\rho_b}{\theta} \frac{\partial (S_1 + S_2)}{\partial t} = k_{sw1} \psi_1 C + k_{sw2} \psi_2 C \tag{2}$$

where t (T; T denotes unit of time) is time, z (L; L denotes units of length) is the direction of mean water flow, C (NL^{-3}; N denotes the bacteria number) is the aqueous phase bacteria concentration, λ (L) is the dispersivity, v (LT^{-1}) is the average pore water velocity, r_{sw} ($NL^{-3}\,T^{-1}$) is the bacteria retention rate, ρ_b (ML^{-3}; M denotes the unit of mass) is the bulk density, θ is the water content, S_1 and S_2 (NM^{-1}) are the solid phase concentrations of bacteria on site 1 and site 2, respectively, and k_{sw1} and k_{sw2} (T^{-1}) are the retention rate

coefficients for site 1 and site 2, respectively. The parameters ψ_1 and ψ_2 are dimensionless Langmuirian blocking functions for sites 1 and 2, respectively, that are given as (Adamczyk et al., 1994)

$$\psi_1 = \left(1-\frac{S_1}{S_{max1}}\right) \qquad \text{and} \qquad \psi_2 = \left(1-\frac{S_2}{S_{max2}}\right) \tag{3}$$

where S_{max1} and S_{max2} (NM^{-1}) are the maximum solid phase concentrations of retained bacteria on site 1 and site 2, respectively. Justification for neglecting bacteria release in the model will be provided later. Bacteria death was negligible over the relatively short duration of these transport experiments, and was therefore not considered in the model.

As will be demonstrated, the number of retention sites that was needed to accurately describe the bacteria BTCs was found to depend on the solution IS. Two retention sites were needed to accurately describe the BTCs when IS < 50 mM, whereas only one site was needed when the IS ≥ 50 mM. The Akaike Information Criterion (AIC) (Akaike, 1974) was also calculated for the BTC data when using the one site and two site retention models. Retention parameters were obtained by fitting to the bacteria BTCs using the nonlinear least squares optimization routine in HYDRUS 1D. Similarly, the value of λ was estimated to be 0.1 cm by fitting HYDRUS-1D output to the BTC of a conservative $NaNO_3$ tracer in the sand packed column.

The fraction of the solid surface area that is available for retention (S_f) was calculated from $S_{max} = S_{max1} + S_{max2}$ as (Kim et al., 2009a; Sasidharan et al., 2014):

$$S_f = \frac{A_c \rho_b S_{max}}{(1-\gamma)A_s} \tag{4}$$

where A_c ($L^2\,N^{-1}$) is the cross sectional area of a cell, A_s (L^{-1}) is the solid surface area per unit volume, and γ is the porosity of a monolayer packing of cells on the solid surface that was taken from the literature to be 0.5 (Johnson and Elimelech, 1995).

The value of the sticking efficiency (α) was determined from $k_{sw} = k_{sw1} + k_{sw2}$ and filtration theory as (Schijven and Hassanizadeh, 2000; Yao et al., 1971):

$$\alpha = \frac{2d_c k_{sw}}{3(1-n)v\eta} \tag{5}$$

where n is the porosity (0.4) and d_c (L) is the collector (median grain) diameter. The value of the single collector-efficiency, η, was calculated using the correlation equation presented by (Tufenkji and Elimelech, 2004a).

3.2. Interaction energy calculations

The total interaction energy between a bacteria and homogeneous collector surface as a function of separation distance (h) was determined as:

$$\Phi_{Total}(h) = \Phi_{vdW}(h) + \Phi_{EDL}(h) + \Phi_{BR}(h) \tag{6}$$

where Φ_{Total} (ML^2T^{-2}) is the total interaction energy, Φ_{vdW} (ML^2T^{-2}) is the van der Waals interaction, Φ_{EDL} (ML^2T^{-2}) is the electrostatic double layer interaction, and Φ_{BR} (ML^2T^{-2}) is the interaction due to Born repulsion. The value of Φ_{vdW} was determined from the expression of Gregory (Gregory, 1981). A combined Hamaker constant value of 4.04×10^{-21} for the bacteria-water-sand system was employed in this study. The value of Φ_{EDL} was calculated using the Hogg-Healy-Fuerstenau expression (Hogg et al., 1966) by employing the measured zeta potentials values in place of surface potentials. The value of Φ_{BR} was calculated using an expression from Ruckenstein and Prieve (1976) by setting the collision diameter at 0.21 nm to achieve a primary minimum depth at 0.157 nm (Van Oss et al., 1988).

Natural solid surfaces like sand grains always contain a wide distribution of physical or chemical surface heterogeneities (Bradford and Torkzaban, 2015; Torkzaban and Bradford, 2016). Bacteria also frequently contain physical (pili or fimbriae) or chemical (protein and lipid membrane) heterogeneity (Huysman and Verstraete, 1993; Walker et al., 2005). However, interaction energy models to account for the full heterogeneity on both the bacteria and the solid-water interface have not yet been published. In this study, the bacterium was therefore considered as homogeneous. Previous researchers have taken this same approach by considering a homogeneous bacterium interacting with a homogeneous sand surface during the Derjaguin-Landau-Verwey-Overbeek interaction energy calculation (Bai et al. 2017; Bayoudh et al., 2009; Dong et al., 2002; Redman et al., 2004).

Bradford and Torkzaban (2015) presented an approach to determine the interaction energy between a homogeneous colloid and a heterogeneous sand grain. This approach was used as a first approximation of the influence of nanoscale heterogeneities on the interaction energy for the bacteria with the grain surface, and employed the same expressions for Φ_{vdW}, Φ_{EDL}, and Φ_{BR} as for the homogeneous collector. In contrast to the homogeneous case, the zone of electrostatic influence (A_z) on the collector surface was now assumed to contain nanoscale roughness and chemical heterogeneity as follows (Bendersky and Davis, 2011).

$$\phi(h) = (1-f_r)\phi_s(h + h_r^n) + f_r\phi_s(h) \tag{7}$$

The dimensionless interaction energy associated with a smooth, nanoscale chemically heterogeneous surface (ϕ_s) is given as (Bendersky and Davis, 2011).

$$\phi_s(h) = (1-f_+)\phi_-(h) + f_+\phi_+(h) \tag{8}$$

where h (L) is the separation distance from the center of A_z at a height h_r^n to a leading face of the colloid center, f_r is the nanoscale roughness fraction with a height equal to h_r^n, and f_+ is the fraction with a positive zeta potential ζ_+. The complementary fractions $(1-f_r)$ and $(1-f_+)$ correspond to a smooth surface and a negative zeta potential ζ_-, respectively. All of the above interaction energies assumed a sphere-plate geometry. A detailed description of the implementation of these equations is given in the literature (Bradford and Torkzaban, 2015).

Specific heterogeneity parameter values used in these calculations included: $f_r = 0.01$; $h_r^n = 33$ nm; $f_+ = 0.1$; and $\zeta_+ = 1$ mV. Note that the value of h_r^n was adapted from Han et al. (2016), whereas other heterogeneity parameters were taken from hypothetical ranges in the literature (Bradford and Torkzaban, 2015).

4. Results and discussion

4.1. Colloid characterization and interaction energy

Table 1 presents the measured zeta potential values of the bacteria and sand grain for the various IS conditions. Zeta potentials of both bacteria and sand surface were negatively charged at the pH of the experiments (5.5–5.8) and as expected, become less negative with increasing IS (−40 to −12 mV for sand and −48 to −8 mV for bacteria). The bacteria cells had an average size of 1231 ± 142 nm in the various solution chemistries, and this confirms the absence of cell aggregation under our experimental conditions. This information was used in interaction energy calculations discussed below.

Table 1 presents calculated interaction energy parameters for a homogeneous bacteria and sand collector under various IS (10, 30, 50, and 300 mM NaCl) and collector heterogeneity conditions. In particular, this table presents values of: (i) the depth of the primary minimum (Φ_{1min}); (ii) the depth of the secondary minimum (Φ_{2min}); (iii) the energy barrier to attachment in the primary minimum ($\Delta\Phi_a = \Phi_{max}/\Phi_{2min}$, where Φ_{max} is the height of the energy barrier); and (iv) the energy barrier to detachment from the primary minimum ($\Delta\Phi_d =$

Table 1
Measured values of zeta potential for *Escherichia coli* bacteria ($\zeta^-_{E.\ coli}$) and sand (ζ^-_{Sand}) in various experimental solution chemistries. Calculated values of interaction energy parameters (the energy barrier to attachment in the primary minimum, $\Delta\Phi_a$; the energy barrier to detachment from the primary minimum, $\Delta\Phi_d$; primary minimum depth, Φ_{1min}; and secondary minimum depth, Φ_{2min}) between a bacterium and a homogeneous or heterogeneous collector surface, respectively.

IS [mM]	ζ^-_{Sand} [mV]	$\zeta^-_{E.\ coli}$ [mV]	Interaction energy between homogeneous colloid and collector surface				Interaction energy between homogeneous colloid and heterogeneous collector surface[§]			
			Φ_{1min} [−]	$\Delta\Phi_a$ [−]	$\Delta\Phi_d$ [−]	Φ_{2min} [−]	Φ_{1min} [−]	$\Delta\Phi_a$ [−]	$\Delta\Phi_d$ [−]	Φ_{2min} [−]
10	−40 ± 4	−48 ± 2	1108 ± 0.2	1380 ± 0.3	271 ± 0.6	−0.51 ± 0.2	3.4 ± 0.4	8.7 ± 0.8	5.1 ± 0.2	−0.21 ± 0.01
30	−37 ± 5	−37 ± 4	627 ± 0.8	851 ± 0.5	221 ± 0.8	−1.8 ± 0.3	1.0 ± 0.4	5.3 ± 0.3	3.8 ± 0.8	−0.33 ± 0.03
50	−25 ± 3	−25 ± 2	−38 ± 0.9	267 ± 0.9	302 ± 0.9	−3.9 ± 0.7	−3.1 ± 0.1	1.4 ± 0.2	4.1 ± 0.2	−0.42 ± 0.02
300	−12 ± 2	−8 ± 3	−511 ± 0.6	0.1 ± 0	511 ± 0.6	−9.3 ± 0.6	−6.0 ± 0.3	0.1 ± 0	6.0 ± 0.3	−0.49 ± 0.05

[§] The zone of influence (A_z) was assumed to contain nanoscale roughness fraction (f_r) = 0.01, with a height (h_r) = 33 nm, a positive zeta potential fraction (f_+) = 0.1 with a positive zeta potential ζ_+ = 1 mV. Interaction energy parameters have been made dimensionless by dividing by the product of the Boltzmann constant and the absolute temperature.

Φ_{max} – Φ_{1min}). Conditions are predicted to be highly unfavorable for bacteria to interact in the primary minimum on a homogeneous collector when the IS ≤50 mM; e.g., $\Delta\Phi_a$ ranges from 267 to 1380 kT. However, the bacteria may still interact in a shallow Φ_{2min} (>–4 kT) under these conditions. Conversely, bacteria attachment in the primary minimum is predicted to be favorable (absence of $\Delta\Phi_a$) at an IS = 300 mM on a homogeneous collector. In this case, the value of $\Delta\Phi_d$ is very large (511 kT) and bacteria interacting in the primary minimum (−511 kT) should be irreversibly retained.

Natural sand grains always exhibit some degree of physical (roughness) and chemical heterogeneity (e.g., metal oxides). For example, scanning electron microscope images shown in Fig. S1 demonstrate significant amounts of roughness on our sand grains. Similarly, Han et al. (2016) reported that AFM analysis of a sand grain demonstrated the presence of an average roughness of ~33 nm. Previous studies have demonstrated that the nanoscale heterogeneity parameters (e.g., f_r, h_r, f_+, and ζ_+) at a particular location on the collector surface can have a large influence on the magnitudes of Φ_{1min}, Φ_{2min}, $\Delta\Phi_a$, and $\Delta\Phi_d$ (Bradford and Torkzaban, 2013; Torkzaban and Bradford, 2016). Consequently, interaction energy calculations in Table 1 that assume a homogeneous sand collector and bacteria are highly idealized, and are not likely to be representative of realistic interaction energies.

Additional interaction energy calculations were therefore conducted to determine hypothetical values of Φ_{1min}, Φ_{2min}, $\Delta\Phi_a$, and $\Delta\Phi_d$ for homogeneous bacteria interacting with a physically and chemically heterogeneous sand surface for all the experimental IS conditions. Selected physical and chemical heterogeneity parameters were taken from the literature (Bradford and Torkzaban, 2012; Bradford and Torkzaban, 2013; Han et al., 2016; Torkzaban and Bradford, 2016); e.g., f_r = 0.01, h_r^n = 33 nm, f_+ = 0.1, and ζ_+ = 1 mV. Table 1 indicates that nanoscale heterogeneity significantly reduced the magnitudes of Φ_{1min}, Φ_{2min}, $\Delta\Phi_a$ and $\Delta\Phi_d$ in comparison with the homogeneous collector surface. For example, the value of $\Delta\Phi_a$ decreased with increasing solution IS and was always <8.7 kT on the heterogeneous collector surface. Interestingly, the value of $\Delta\Phi_d$ was also rather small (<5.1 kT), especially at intermediate IS (30 and 50 mM) conditions. The Maxwellian kinetic energy model predicts a rapid increase in the probability of cells to diffuse into or out of a primary minimum when $\Delta\Phi_a$ and $\Delta\Phi_d$ are <10 kT (Bradford and Torkzaban, 2012; Simoni et al., 1998; Torkzaban and Bradford, 2016; Wang et al., 2016). These relatively low values of $\Delta\Phi_a$ (0.1–8.7 kT) and $\Delta\Phi_d$ (5.1–6.0 kT), therefore, indicate that reversible primary minimum interactions are possible under all of the IS conditions.

4.2. Retention of bacteria

Fig. 1 shows observed and fitted BTCs for the bacteria under the various IS (10, 30, 50, and 300 mM) and flow velocity (1, 5, and 50 m day^{-1}) conditions. The normalized effluent concentrations C/C_0 (where C_0 is the influent bacteria concentration and C is the effluent concentration) were plotted as a function of pore volumes. Table 2 presents experimental mass balance (M_{BTC}, M_s, M_{III}, M_{IV}, M_V, and M_{irr}) information and Table 3 presents fitted (k_{sw1}, k_{sw2}, S_{max1}/C_0, and S_{max2}/C_0) or calculated model parameters (α, η, and S_f), and the Pearson's correlation coefficient (R^2) for the goodness of model fit. Values of AIC indicated that the two-site retention model was justified for the IS = 10 and 30 mM data, whereas the one site retention model was sufficient for the IS = 50 and 300 mM data. This observation likely reflects a non-uniform distribution of bacteria retention sites when the IS = 10 and 30 mM, and a more uniform distribution of sites under higher IS conditions that are more favorable for retention. However, k_{sw1} was orders of magnitude higher than k_{sw2} when the IS = 10 and 30 mM. Simulation results always provided an acceptable description of the BTCs when IS ≤50 mM (R^2 > 0.91), and negligible cell release occurred during Phase II.

Fitted parameter values are not presented for the IS = 300 mM and v = 1 and 5 m day^{-1} experiments because a unique determination of retention parameters was not possible due to the very low effluent bacteria concentrations and the negligible rising limb of the BTC. Previous researchers reported the complete retention of biocolloids such as bacteria in packed column scale studies at highly favorable solution chemistry (i.e., IS >100 mM) and constant flow rate conditions (Kim et al., 2009a). However, an improved understanding of the velocity dependency of bacteria deposition under such a highly favorable condition is needed to predict biocolloid transport in wastewater treatment plants, salt-water intrusion zones, and salt contaminated or brackish groundwater systems.

Fig. 2a summarizes the BTCs results from Fig. 1 by presenting a plot of the percentage of bacteria mass retained on the solid phase (M_s = 100-M_{BTC}) as a function of velocity (1, 5 and 50 m day^{-1}) and solution IS (10, 30, 50, and 100 mM). As expected, bacteria retention and k_{sw1} (Tables 2 and 3, respectively) dramatically increased with increasing IS at a given flow velocity due to a reduction in $\Delta\Phi_a$ (Table 1). When the velocity was increased from 1 to 5 and 50 m day^{-1} the retention of bacteria at a given IS was reduced. Furthermore, this velocity dependency of M_s was a function of IS. In particular, velocity had a greater influence on bacteria retention at intermediate IS (30 and 50 mM), then at lower (10 mM) or higher (300 mM) IS conditions. The primary objective of this research is to better understand this velocity effect on bacteria retention.

Colloid filtration theory has been developed to predict the value of k_{sw} under different physicochemical conditions (Yao et al., 1971). This theory considers that k_{sw} is proportional to the product of η and α that account for mass transfer and adhesion, respectively. The value of α is assumed in colloid filtration theory to be constant for different velocities at a given IS because the interaction energy does not change. Consequently, changes in k_{sw} with velocity at a given IS are predicted to occur solely due to differences in mass transfer. Consistent with colloid filtration theory predictions the value of k_{sw} (Table 3) increased with increasing fluid velocity at a given IS (Johnson and Tong, 2006). The observed decrease in retention (M_s) with increasing velocity at a given IS (Fig. 2a) is therefore predicted by colloid filtration theory to be controlled by a decrease in the advection controlled residence time at a higher velocity.

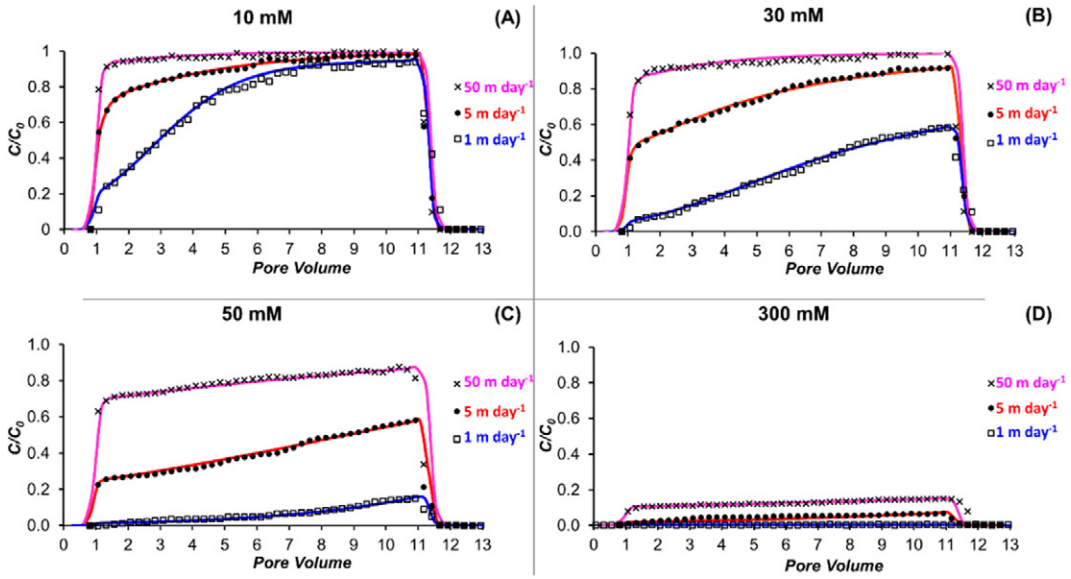

Fig. 1. Observed effluent concentrations (marker) and corresponding model fits (solid line) for representative effluent concentrations of *E. coli* bacteria for experiments conducted at IS of (A) 10 mM, (B) 30 mM, (C) 50 mM and (D) 300 mM, at flow velocity = 1, 5 and 50 m day^{-1}, temperature = 20 °C and pH = 5.8. Table 3 provides the values of fitted parameters (k_{sw1}, k_{sw2}, S_{max1}, and S_{max2}).

Table 3 presents values of α that were determined from fitted values of k_{sw} and colloid filtration theory (Eq. (5)), and values of S_f that were calculated from fitted values of S_{max} (Eq. (4)). In contrast to the colloid filtration theory assumption, values of α and S_f decreased with increasing velocity at a given IS. Indeed, values α and S_f tended to follow the same trend as M_s, in Fig. 2a. In particular, the velocity dependency of α and S_f are greater at intermediate IS (30 and 50 mM), than at the lower (10 mM) IS condition. Other researchers have similarly reported that values of α and S_f decrease or were constant with increasing velocity at a given IS (Kim and Lee, 2014; Shen et al., 2010; Tong and Johnson, 2006; Torkzaban et al., 2010; Torkzaban et al., 2008; Walker et al., 2004). However, the coupled role of velocity and IS on α and S_f have not yet been systematically studied. An explanation for the observed velocity dependency of α and S_f will be given later in this manuscript.

4.3. Release of bacteria

Fig. 3 shows plots of the bacteria concentration in the column effluent during Phase III when the velocity was systematically increased up to 100 or 150 m day^{-1} under constant IS (10, 30, 50 and 300 mM) conditions. This figure also shows cell release during Phase IV, which included a 24-h flow interruption followed by continued flushing with the same solution IS at 5 m day^{-1}. Pulses of released bacteria were observed with each increase in flow velocity during Phase III, and especially following the flow interruption during Phase IV. In addition to velocity, the amount of cell release during Phases III and IV also depended on the solution IS i.e. intermediate IS (30 and 50 mM) had a greater influence than low (10 mM) and high (300 mM) ionic strength (Table 2). Fig. S2 summarizes mass balance information from Phase III of the release experiments by plotting the fraction of retained cells that was not released (f_{nr}) as a function of flow velocity for the various IS conditions. This figure indicates that $f_{nr} = (M_s - M_{III}) / M_s$ was >0.93 after completion of Phase III when the velocity was increased up to 100 or 150 m day^{-1}. Greater amounts of cell release occurred during Phase IV following the 24-h flow interruption. However, the value of $f_{nr} = (M_s - M_{III} - M_{IV}) / M_s$ still ranged from 0.78 to 0.97 (Table 2).

Table 2
Experimental conditions and mass balance information from the column experiments. Here M_{BTC}, M_s = 100-M_{BTC}, M_{III}, M_{IV}, M_V, and M_{irr} = (100-M_{BTC}-M_{III}-M_{IV}-M_V) denote the percentage of the injection bacteria that was recovered in the breakthrough curve, on the solid phase, with the increasing velocity release Phase III, following the flow interruption release Phase IV, after excavation of the sand during Phase V, and irreversibly retained on the solid following completion of Phases I–V, respectively.

Velocity [m day^{-1}]	IS [mM]	M_{BTC} [%]	M_s [%]	M_{III} [%]	M_{IV} [%]	M_V [%]	M_{irr} [%]
1	10	70	30	2	1	23	4
5		85	15	0.03	3	11	1
50		91	9	0.03	0.002	8	1
1	30	32	68	1	5	52	10
5		72	28	1	5	19	3
50		89	11	0.03	0.02	9	2
1	50	6	94	2	2	74	16
5		38	62	2	4	46	10
50		69	31	1	1	26	3
1	300	0	100	0.4	2	77	21
5		5	95	2	2	75	16
50		12	88	1	4	72	11

Table 2 shows bacteria mass balance information following excavation of the sand in the columns in an excess solution having the same IS as the transport experiments (M_V). The vast majority of the retained bacteria were recovered during this excavation process (Table 2); i.e., the value of $(M_{III} + M_{IV} + M_V) / M_s$ ranged from 0.79 to 0.94. However, a small fraction of the bacteria mass was unaffected by the excavation step and remained attached to the sand surface (M_{irr}). Fig. 2b shows a plot of $M_{irr} = 100 - M_{BTC} - M_{III} - M_{IV} - M_V$ as a function of velocity (Phase I) and constant IS conditions. The presence of these irreversibly retained bacteria on the excavated sand grains is apparent in the scanning electron microscope images shown in Fig. S1b. Interestingly, the value of M_s in Fig. 2a and the value of M_{irr} in Fig. 2b follow similar trends with velocity and IS. In particular, the value of M_{irr} increases with IS and decreases with increasing velocity. Velocity has the greatest influence on the value of M_{irr} at intermediate IS (30 and 50 mM), and less of an influence at lower (10 mM) and higher (300 mM) IS conditions.

4.4. Role of residence time

The residence time of a bacterium at a particular location on the sand surface is inversely related to the velocity. An increase in the bacteria residence time at a particular location on the collector surface (e.g., a decrease in velocity) increases the probability that random Brownian motion will achieve a sufficient kinetic energy to overcome $\Delta\Phi_a$ and thereby increase the adhesive strength. The observed increase in the irreversible bacteria mass with decreasing velocity and increasing IS (Fig. 2b) is consistent

Table 3
Experimental conditions and fitted model parameters for column experiments shown in Figs. 1–4.

Velocity [m day^{-1}]	IS [mM]	k_{sw1} [min^{-1}]	k_{sw2} [min^{-1}]	α	η	S_{max1}/C_0 [cm^3 g^{-1}]	S_{max2}/C_0 [cm^3 g^{-1}]	S_f [%]	R^2 [%]
1	10	1.1×10^{-2}	4.9×10^{-4}	0.097	0.048	0.45	0.52	9.0	98.9
5		1.3×10^{-2}	1.1×10^{-2}	0.089	0.015	0.02	0.24	2.7	97.5
50		2.4×10^{-2}	7.2×10^{-4}	0.035	0.004	6.2×10^{-6}	0.04	0.9	96.1
1	30	1.6×10^{-2}	6.8×10^{-3}	0.156	0.048	0.49	2.7	24.3	99.4
5		1.7×10^{-2}	9.7×10^{-3}	0.101	0.015	0.25	0.46	7.3	96.1
50		3.4×10^{-2}	1.5×10^{-2}	0.070	0.004	0.03	0.07	1.8	96.0
1	50	2.9×10^{-2}	NA[a]	0.196	0.048	3.9	NA[a]	39.4	98.4
5		4.9×10^{-2}	NA[a]	0.187	0.015	2.5	NA[a]	25.5	94.5
50		8.4×10^{-2}	NA[a]	0.123	0.004	0.82	NA[a]	8.6	91.4
1	300	ND[b]	ND[b]	ND[b]	0.048	ND[b]	ND[b]	ND[b]	ND[b]
5		ND[b]	ND[b]	ND[b]	0.015	ND[b]	ND[b]	ND[b]	ND[b]
50		3.7×10^{-1}	NA[a]	0.543	0.004	2.6	NA[a]	26.4	88.2

[a] NA = Not applicable.
[b] ND = Not determined.

with an increasing adhesive strength because the probability to diffuse over $\Delta\Phi_a$ increases with the residence time and $\Delta\Phi_a$ is smaller at higher IS ($\Delta\Phi_a = 0.1$ kT for 300 mM), respectively. The increased sensitivity of the amount of irreversibly retained bacteria to velocity at intermediate IS (30 and 50 mM) in Fig. 2b is also consistent with the residence time explanation because the value of $\Delta\Phi_d$ is smaller ($\Delta\Phi_d = 3.8$ and 4.1 kT for 30 and 50 mM, respectively) under these conditions and this produces a greater probability of cell release via diffusion or hydrodynamic removal. In addition, the minor amounts of cell release following a 24-h flow interruption ($M_{IV} \leq 5\%$) suggest the presence of a relative strong primary minimum interaction that does not readily allow diffusive cell release.

Other researchers have similarly reported that the adhesive interaction increases with the residence time (Mondon et al., 2003; Stuart and Hlady, 1995; Vadillo-Rodriguez et al., 2004; Xu and Logan, 2006). For example, Xu and Logan (2006) reported that the adhesive strength between a latex colloid and glass surface consistently increased with IS (1–100 mM) and residence time (1–100 s). Their results also demonstrated that the presence of various functional groups and protein (nanoscale chemical heterogeneity) on both collector and colloid surface produced a very strong adhesive force via chemical and/or electrostatic bonding at residence time <1 s (Xu and Logan, 2006). Similarly, Vadillo-Rodriguez et al. (2004) reported that the adhesive force between a hydrophilic, negatively charged AFM tip and *Streptococcus thermophiles* bacteria cell surface was strengthened with residence time (100 s) and observed multiple adhesion events before reaching the maximum adhesion strength. These observations were attributed to the reversible attachment of bacteria in the secondary energy minimum and the subsequent anchoring of their extracellular polymeric substances to the solid surface that helps to surpass the energy barrier (Vadillo-Rodriguez et al., 2004). Note that these studies did not relate their findings to transport velocity and to random Brownian motion. Thus, the findings from this study reveals that the transport velocity is inversely related to the residence time, and an increase in the bacteria residence time at a particular location on the collector surface will increase the probability that random Brownian motion will achieve a sufficient kinetic energy to overcome the energy barrier to the primary minimum and thereby increase the adhesive strength. This implies that greater bacteria retention and less release many occur at lower water velocities with larger residence times and adhesive strength.

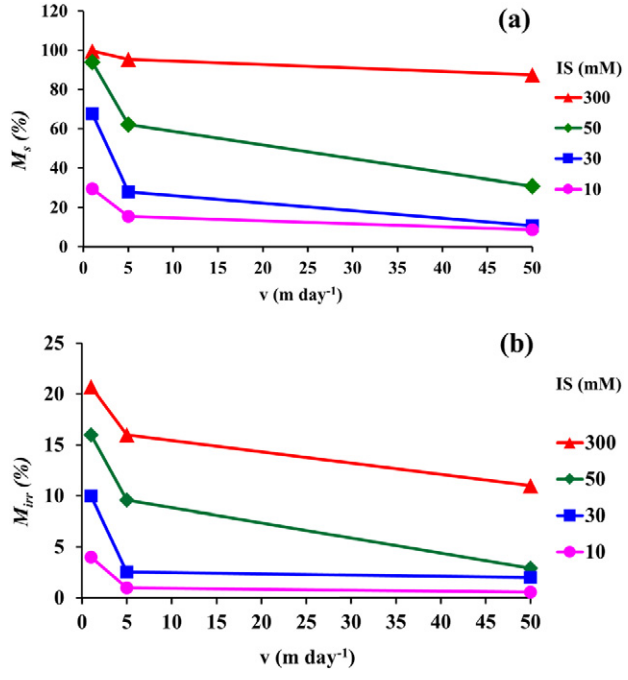

Fig. 2. Plots of the percentage of bacteria mass retained on the solid phase (M_s) (Fig. 2a) and the percentage of injected cells that were irreversibly retained (M_{irr}) (Fig. 2b) as a function of velocity (Phase I) and solution IS.

4.5. Role of torque balance

Bacteria retention and release at a particular location depends on force and torque balances at a particular location. The applied hydrodynamic (T_H) and resisting adhesive (T_A) torques are functions of the water velocity and the adhesive strength, respectively, as well as their lever arms (Bradford et al., 2011b; Li et al., 2005; Torkzaban et al., 2007). The lever arm is defined as the perpendicular distance from the axis of rotation to the line of action of the force (Torkzaban et al., 2007). Bacteria immobilization occurs when $T_A \geq T_H$, whereas hydrodynamic removal occurs when $T_A < T_H$. The negligible amount of bacteria release ($M_{III} < 2\%$) with increasing water velocity during Phase III (Fig. S2) indicates that $T_A \geq T_H$, even when the velocity was up to 100 or 150 m day^{-1}. This can only occur if the adhesive force is very strong or if the lever arms for T_A and T_H are large and small, respectively. Although Fig. 2b indicates that the adhesive strength increased with the residence time (lower velocity) (e.g., M_{irr} increases with decreasing velocity), Table 1 shows that Φ_{1min} (≤–6 kT) and Φ_{2min} (≤–0.49 kT) are expected to be shallow on heterogeneous collector surfaces. Conversely, the lever arms on natural sand surfaces that exhibit significant amounts of roughness (Fig. S1) are controlled by the grain surface topography in column systems. In particular, lever arms associated with T_A and T_H are large and small, respectively, at microscopic roughness locations and grain-grain contacts. Consequently, enhanced bacteria and colloid retention has been experimentally observed and theoretically predicted at these locations, especially at lower IS and higher velocity conditions (Bradford et al., 2006; Bradford et al., 2013). Note that the T_H is equal

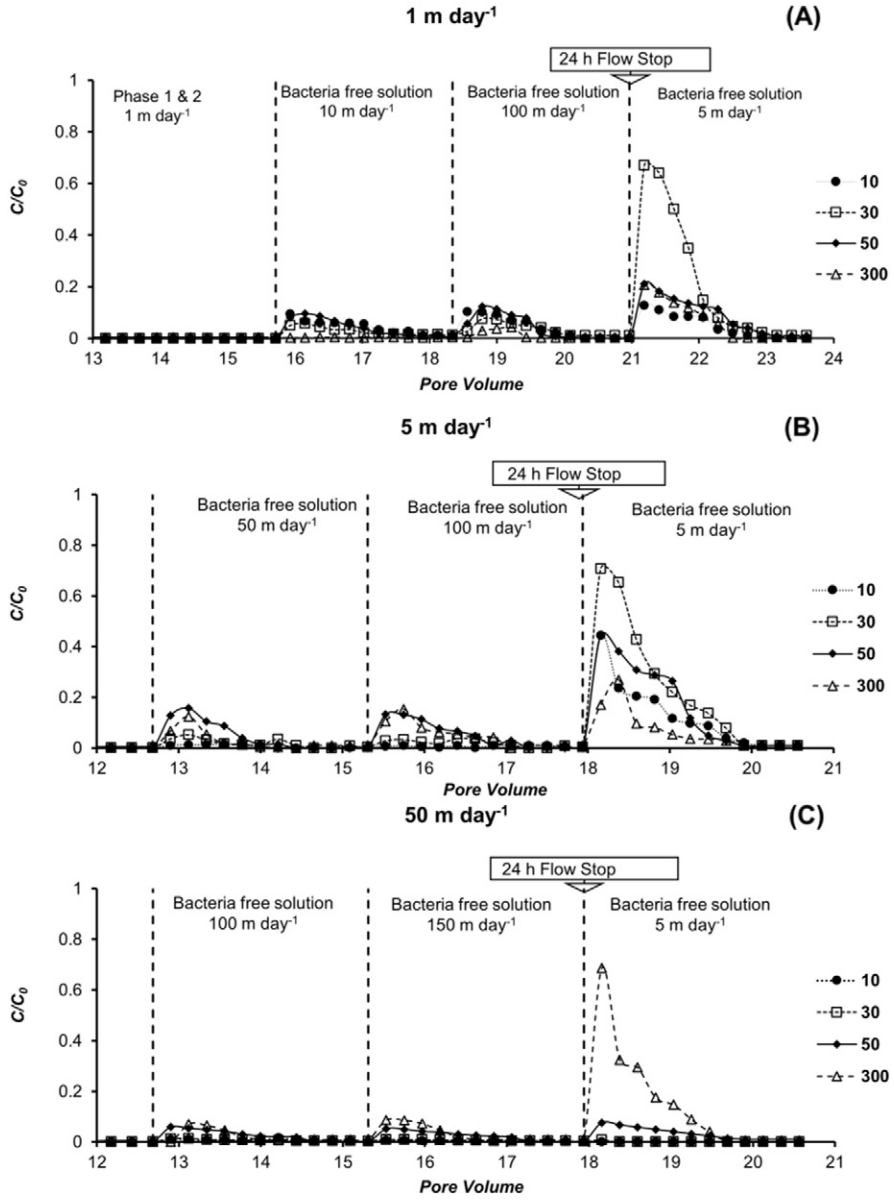

Fig. 3. Observed effluent concentrations of *E. coli* bacteria during Phase III (successive increase in flow velocity) and Phase IV (24 h flow interruption and resumed the flow at 5 m day^{-1}) at the indicated solution IS when the pore-water velocity of Phase I and II was (A) 1 m day^{-1} (B) 5 m day^{-1}, and (C) 50 m day^{-1}. Associated BTCs from Phases I and II are given in Fig. 1.

to zero when the roughness height is greater than the colloid radius (Bradford et al., 2013). Consequently, bacteria release is predicted to be independent of the water velocity at these locations and this explains the negligible release of retained bacteria in Phase III and IV. The dominant role of roughness on the torque balance is also consistent with the fact that > 79% of the retained cells were recovered following excavation into excess solution at the same IS that was continuously mixed such that the lever arms were not constant (Table 2).

4.6. Velocity and IS dependence of α and S_f

The above information provides an explanation for the observed velocity dependency of α and S_f (Table 3). In particular, increases in velocity produces a decrease in α and S_f by increasing the applied hydrodynamic torque on relatively smooth portions of the collector surface and by decreasing the residence time that cells can diffuse into a primary minimum. This velocity dependency also is a function of the solution IS because of its influence on $\Delta\Phi_a$ and $\Delta\Phi_d$ (Table 1) for heterogeneous collector surfaces. Values of α (0.035) and S_f (0.9%) were lowest at IS = 10 mM because $\Delta\Phi_a$ (8.7 kT) and $\Delta\Phi_d$ (5.1 kT) were highest under these conditions and this indicates a low probability for cells to diffuse into or out of the primary minimum. Values of α and S_f increase with IS because $\Delta\Phi_a$ decreases and this increases the probability for more primary minimum interactions, especially at low velocities with a greater residence time. The primary minimum interactions are more susceptible to removal via diffusive and hydrodynamic forces at intermediate IS conditions because of their low value of $\Delta\Phi_d$ (3.8 and 4.1 kT). Consequently, the velocity dependency of α and S_f was greater under these conditions. The values of α (≤0.196) and S_f (≤39.4%) were always much less than unity, even when the IS = 300 mM, because nanoscale roughness produces shallow primary minimum interactions that were susceptible to diffusive and hydrodynamic removal unless the lever arms were controlled by microscopic roughness locations.

5. Conclusions

Bacteria transport and retention studies are typically interpreted in terms of colloid filtration theory, which assumes that immobilization

parameters are independent of v. A number of publications have previously indicated that this assumption can be violated, but have not yet considered all relevant factors that contribute to the velocity dependency of retention and release parameters. This study was therefore designed to investigate the causes and complexities associated with the velocity dependency of *E. coli* retention and release parameters under different IS conditions.

The main observations and conclusions from this study are that α, S_f, and M_{irr} increased with increasing IS and decreasing v, and the velocity dependency was greatest at intermediate IS. The increase in α, S_f, and M_{irr} with increasing IS occurs due to a reduction or elimination of the energy barrier and stronger primary minimum interactions. The increase in α, S_f, and M_{irr} with a decrease in v was explained by lower hydrodynamic forces that satisfy the torque balance on more regions of the grain surface. In addition, a decrease in v also increases the residence time for the cells and thereby increases the probability that cells can diffuse over the energy barrier into a deeper minimum in the interaction energy. Consequently, an increase in the residence time produced stronger adhesive interactions, and larger values of M_{irr}. The velocity dependency of retention parameters was greatest at intermediate IS conditions because there was a greater probability to diffuse over their small energy barriers with increasing residence time (lower velocities). Findings from this study therefore provide an explanation for the observed velocity dependency of α and S_f that is not allowed in colloid filtration theory.

Large variations in v from 1 to 150 m day^{-1} had a negligible influence on cell release, whereas the vast majority (>79%) of retained cells could be recovered after excavation of the sand. The negligible amount of bacteria release with increasing v indicates that $T_A \geq T_H$. This was attributed to the controlling influence of lever arms in determining T_A and T_H at microscopic roughness locations and grain-grain contacts points because the minima in the interaction energy was calculated to be shallow on rough grain surfaces. In addition, continuously changing lever arms in excavated sand can also explain the recovery of the vast majority of retained cells. This research demonstrates that the velocity and the resultant residence time have a significant role in determining the retention parameters but had a negligible effect on cell release. This finding will help to determine parameters such as injection and recovery pumping velocity for the efficient running of natural and engineered water recycling applications such as Managed Aquifer Recharge.

Notes

The authors declare no competing financial interest.

Acknowledgements

Funding for this research was provided by the National Centre for Groundwater Research and Training (Ph.D. Research Scholarship awarded to S. Sasidharan, 2012–2016), an Australian Government initiative, supported by the Australian Research Council (ARC) and the National Water Commission (NWC). The project was completed in collaboration with CSIRO Land and Water program and the Flinders University of South Australia. The work was conducted in the CSIRO Laboratories at the Waite Campus, Adelaide, South Australia.

Appendix A. Supplementary data

Supplementary data to this article can be found online at http://dx.doi.org/10.1016/j.scitotenv.2017.06.091.

References

Adamczyk, Z., Siwek, B., Zembala, M., Belouschek, P., 1994. Kinetics of localized adsorption of colloid particles. Adv. Colloid Interf. Sci. 48, 151–280.
Ahmadi, G., Guo, S., Zhang, X., 2007. Particle adhesion and detachment in turbulent flows including capillary forces. Part. Sci. Technol. 25, 59–76.
Akaike, H., 1974. A new look at the statistical model identification. Automatic Control, IEEE Transactions on 19, 716–723.
Bai, H., Cochet, N., Pauss, A., Lamy, E., 2017. DLVO, hydrophobic, capillary and hydrodynamic forces acting on bacteria at solid-air-water interfaces: their relative impact on bacteria deposition mechanisms in unsaturated porous media. Colloids Surf. B: Biointerfaces.
Bayoudh, S., Othmane, A., Mora, L., Ben Ouada, H., 2009. Assessing bacterial adhesion using DLVO and XDLVO theories and the jet impingement technique. Colloids Surf. B: Biointerfaces 73, 1–9.
Bendersky, M., Davis, J.M., 2011. DLVO interaction of colloidal particles with topographically and chemically heterogeneous surfaces. J. Colloid Interface Sci. 353, 87–97.
Bergendahl, J., Grasso, D., 2000. Prediction of colloid detachment in a model porous media: hydrodynamics. Chem. Eng. Sci. 55, 1523–1532.
Bolster, C.H., Mills, A.L., Hornberger, G., Herman, J., 2000. Effect of intra-population variability on the long-distance transport of bacteria. Groundwater 38, 370–375.
Bolster, C.H., Mills, A.L., Hornberger, G.M., Herman, J.S., 2001. Effect of surface coatings, grain size, and ionic strength on the maximum attainable coverage of bacteria on sand surfaces. J. Contam. Hydrol. 50, 287–305.
Bradford, S.A., Torkzaban, S., 2012. Colloid adhesive parameters for chemically heterogeneous porous media. Langmuir 28, 13643–13651.
Bradford, S.A., Torkzaban, S., 2013. Colloid interaction energies for physically and chemically heterogeneous porous media. Langmuir 29, 3668–3676.
Bradford, S.A., Torkzaban, S., 2015. Determining parameters and mechanisms of colloid retention and release in porous media. Langmuir 31, 12096–12105.
Bradford, S.A., Simunek, J., Walker, S.L., 2006. Transport and straining of *E. coli* O157:H7 in saturated porous media. Water Resour. Res. 42 n/a-n/a.
Bradford, S.A., Torkzaban, S., Leij, F., Šimůnek, J., van Genuchten, M.T., 2009. Modeling the coupled effects of pore space geometry and velocity on colloid transport and retention. Water Resour. Res. 45 n/a-n/a.
Bradford, S.A., Torkzaban, S., Simunek, J., 2011a. Modeling colloid transport and retention in saturated porous media under unfavorable attachment conditions. Water Resour. Res. 47 n/a-n/a.
Bradford, S.A., Torkzaban, S., Wiegmann, A., 2011b. Pore-scale simulations to determine the applied hydrodynamic torque and colloid immobilization. Vadose Zone J. 10, 252.
Bradford, S.A., Torkzaban, S., Kim, H., Simunek, J., 2012. Modeling colloid and microorganism transport and release with transients in solution ionic strength. Water Resour. Res. 48 n/a-n/a.
Bradford, S.A., Torkzaban, S., Shapiro, A., 2013. A theoretical analysis of colloid attachment and straining in chemically heterogeneous porous media. Langmuir 29, 6944–6952.
Burdick, G.M., Berman, N.S., Beaudoin, S.P., 2001. Describing hydrodynamic particle removal from surfaces using the particle Reynolds number. J. Nanopart. Res. 3, 453–465.
Cushing, R.S., Lawler, D.F., 1998. Depth filtration: fundamental investigation through three-dimensional trajectory analysis. Environ. Sci. Technol. 32, 3793–3801.
Dong, H., Onstott, T.C., Ko, C.-H., Hollingsworth, A.D., Brown, D.G., Mailloux, B.J., 2002. Theoretical prediction of collision efficiency between adhesion-deficient bacteria and sediment grain surface. Colloids Surf. B: Biointerfaces 24, 229–245.
Elimelech, M., 1994. Effect of particle size on the kinetics of particle deposition under attractive double layer interactions. J. Colloid Interface Sci. 164, 190–199.
Elimelech, M., O'Melia, C.R., 1990. Kinetics of deposition of colloidal particles in porous media. Environ. Sci. Technol. 24, 1528–1536.
Elimelech, M., Chen, W.H., Waypa, J.J., 1994. Measuring the zeta (electrokinetic) potential of reverse osmosis membranes by a streaming potential analyzer. Desalination 95, 269–286.
Elimelech, M., Jia, X., Gregory, J., Williams, R., 1998. Particle Deposition & Aggregation: Measurement, Modelling and Simulation: Butterworth-Heinemann.
Gannon, J., Tan, Y.H., Baveye, P., Alexander, M., 1991. Effect of sodium chloride on transport of bacteria in a saturated aquifer material. Appl. Environ. Microbiol. 57, 2497–2501.
Goldman, A.J., Cox, R.G., Brenner, H., 1967. Slow viscous motion of a sphere parallel to a plane wall—I motion through a quiescent fluid. Chem. Eng. Sci. 22, 637–651.
Gregory, J., 1981. Approximate expressions for retarded van der waals interaction. J. Colloid Interface Sci. 83, 138–145.
Han, Y., Hwang, G., Kim, D., Bradford, S.A., Lee, B., Eom, I., et al., 2016. Transport, retention, and long-term release behavior of ZnO nanoparticle aggregates in saturated quartz sand: role of solution pH and biofilm coating. Water Res. 90, 247–257.
Hemmerle, J., Altmann, S.M., Maaloum, M., Horber, J.K., Heinrich, L., Voegel, J.C., et al., 1999. Direct observation of the anchoring process during the adsorption of fibrinogen on a solid surface by force-spectroscopy mode atomic force microscopy. U S A]–>Proc. Natl. Acad. Sci. U. S. A. 96, 6705–6710.
Hendry, M.J., Lawrence, J.R., Maloszewski, P., 1999. Effects of velocity on the transport of two bacteria through saturated sand. Ground Water 37, 103–112.
Hogg, R., Healy, T.W., Fuerstenau, D.W., 1966. Mutual coagulation of colloidal dispersions. Trans. Faraday Soc. 62, 1638.
Huysman, F., Verstraete, W., 1993. Effect of cell surface characteristics on the adhesion of bacteria to soil particles. Biol. Fertil. Soils 16, 21–26.
Johnson, P.R., Elimelech, M., 1995. Dynamics of colloid deposition in porous media: blocking based on random sequential adsorption. Langmuir 11, 801–812.
Johnson, W.P., Tong, M., 2006. Observed and simulated fluid drag effects on colloid deposition in the presence of an energy barrier in an impinging jet system. Environ. Sci. Technol. 40, 5015–5021.
Johnson, K., Kendall, K., Roberts, A., 1971. Surface energy and the contact of elastic solids. Proceedings of the Royal Society of London A: Mathematical, Physical and Engineering Sciences 324, 301–313 The Royal Society.
Johnson, W.P., Li, X., Yal, G., 2007. Colloid retention in porous media: mechanistic confirmation of wedging and retention in zones of flow stagnation. Environ. Sci. Technol. 41, 1279–1287.
de Kerchove, A.J., Elimelech, M., 2008. Bacterial swimming motility enhances cell deposition and surface coverage. Environ. Sci. Technol. 42, 4371–4377.
Kim, C., Lee, S., 2014. Effect of seepage velocity on the attachment efficiency of TiO2 nanoparticles in porous media. J. Hazard. Mater. 279, 163–168.
Kim, H.N., Bradford, S.A., Walker, S.L., 2009a. *Escherichia coli* O157:H7 transport in saturated porous media: role of solution chemistry and surface macromolecules. Environ. Sci. Technol. 43, 4340–4347.

Kim, H.N., Hong, Y., Lee, I., Bradford, S.A., Walker, S.L., 2009b. Surface characteristics and adhesion behavior of *Escherichia coli* O157:H7: role of extracellular macromolecules. Biomacromolecules 10, 2556–2564.
Kuznar, Z.A., Elimelech, M., 2007. Direct microscopic observation of particle deposition in porous media: role of the secondary energy minimum. Colloids Surf. A Physicochem. Eng. Asp. 294, 156–162.
Li, X., Johnson, W.P., 2005. Nonmonotonic variations in deposition rate coefficients of microspheres in porous media under unfavorable deposition conditions. Environ. Sci. Technol. 39, 1658–1665.
Li, X., Zhang, P., Lin, C.L., Johnson, W.P., 2005. Role of hydrodynamic drag on microsphere deposition and re-entrainment in porous media under unfavorable conditions. Environ. Sci. Technol. 39, 4012–4020.
Liu, Y., Yang, C.H., Li, J., 2007. Influence of extracellular polymeric substances on *Pseudomonas aeruginosa* transport and deposition profiles in porous media. Environ. Sci. Technol. 41, 198–205.
Ma, H., Hradisky, M., Johnson, W.P., 2013. Extending applicability of correlation equations to predict colloidal retention in porous media at low fluid velocity. Environ. Sci. Technol. 47, 2272–2278.
Malvern Instruments Ltd. Zetasizer Nano Series User Manual, 2016, 2004. Malvern Instruments Ltd, United Kingdom.
Massoudieh, A., Lu, N., Liang, X., Nguyen, T.H., Ginn, T.R., 2013. Bayesian process-identification in bacteria transport in porous media. J. Contam. Hydrol. 153, 78–91.
McCaulou, D.R., Bales, R.C., Arnold, R.G., 1995. Effect of temperature controlled motility on transport of bacteria and microspheres through saturated sediment. Water Resour. Res. 31, 271–280.
Meinders, J.M., van der Mei, H.C., Busscher, H.J., 1994. Physicochemical aspects of deposition of *Streptococcus thermophilus* B to hydrophobic and hydrophilic substrata in a parallel plate flow chamber. J. Colloid Interface Sci. 164, 355–363.
Meinders, J.M., van der Mei, H.C., Busscher, H.J., 1995. Deposition efficiency and reversibility of bacterial adhesion under flow. J. Colloid Interface Sci. 176, 329–341.
Messina, F., Marchisio, D.L., Sethi, R., 2015. An extended and total flux normalized correlation equation for predicting single-collector efficiency. J. Colloid Interface Sci. 446, 185–193.
Mondon, M., Berger, S., Ziegler, C., 2003. Scanning-force techniques to monitor time-dependent changes in topography and adhesion force of proteins on surfaces. Anal. Bioanal. Chem. 375, 849–855.
Morales, I., Amador, J.A., Boving, T., 2015. Bacteria transport in a soil-based wastewater treatment system under simulated operational and climate change conditions. J. Environ. Qual. 44, 1459–1472.
Nelson, K.E., Ginn, T.R., 2011. New collector efficiency equation for colloid filtration in both natural and engineered flow conditions. Water Resour. Res. 47.
O'Neill, M.E., 1968. A sphere in contact with a plane wall in a slow linear shear flow. Chem. Eng. Sci. 23, 1293–1298.
Rajagopalan, R., Tien, C., 1976. Trajectory analysis of deep-bed filtration with the sphere-in-cell porous media model. AICHE J. 22, 523–533.
Redman, J.A., Walker, S.L., Elimelech, M., 2004. Bacterial adhesion and transport in porous media: role of the secondary energy minimum. Environ. Sci. Technol. 38, 1777–1785.
Ruckenstein, E., Prieve, D.C., 1976. Adsorption and desorption of particles and their chromatographic separation. AICHE J. 22, 276–283.
Saffman, P.G., 2006. The lift on a small sphere in a slow shear flow. J. Fluid Mech. 22, 385.
Sasidharan, S., Torkzaban, S., Bradford, S.A., Dillon, P.J., Cook, P.G., 2014. Coupled effects of hydrodynamic and solution chemistry on long-term nanoparticle transport and deposition in saturated porous media. Colloids Surf. A Physicochem. Eng. Asp. 457, 169–179.
Sasidharan, S., Torkzaban, S., Bradford, S.A., Cook, P.G., Gupta, V.V., 2017. Temperature dependency of virus and nanoparticle transport and retention in saturated porous media. J. Contam. Hydrol. 196, 10–20.
Schijven, J.F., Hassanizadeh, S.M., 2000. Removal of viruses by soil passage: overview of modeling, processes, and parameters. Crit. Rev. Environ. Sci. Technol. 30, 49–127.
Schulze-Makuch, D., Bowman, R.S., Pillai, S.D., Guan, H., 2003. Field evaluation of the effectiveness of surfactant modified zeolite and iron-oxide-coated sand for removing viruses and bacteria from ground water. Groundwater Monitoring & Remediation 23, 68–74.
Sharma, M.M., Chamoun, H., Sarma, D.S.H.S.R., Schechter, R.S., 1992. Factors controlling the hydrodynamic detachment of particles from surfaces. J. Colloid Interface Sci. 149, 121–134.
Shellenberger, K., Logan, B.E., 2002. Effect of molecular scale roughness of glass beads on colloidal and bacterial deposition. Environ. Sci. Technol. 36, 184–189.
Shen, C., Huang, Y., Li, B., Jin, Y., 2010. Predicting attachment efficiency of colloid deposition under unfavorable attachment conditions. Water Resour. Res. 46 n/a-n/a.
Shen, C., Wang, L.-P., Li, B., Huang, Y., Jin, Y., 2012. Role of surface roughness in chemical detachment of colloids deposited at primary energy minima. Vadose Zone J. 11 (0).
Shen, C., Lazouskaya, V., Zhang, H., Li, B., Jin, Y., Huang, Y., 2013. Influence of surface chemical heterogeneity on attachment and detachment of microparticles. Colloids Surf. A Physicochem. Eng. Asp. 433, 14–29.
Simoni, S.F., Harms, H., Bosma, T.N.P., Zehnder, A.J.B., 1998. Population heterogeneity affects transport of bacteria through sand columns at low flow rates. Environ. Sci. Technol. 32, 2100–2105.
Simoni, S.F., Bosma, T.N.P., Harms, H., Zehnder, A.J.B., 2000. Bivalent cations increase both the subpopulation of adhering bacteria and their adhesion efficiency in sand columns. Environ. Sci. Technol. 34, 1011–1017.
Simunek JvG, M.Th., Sejna, M., 2005. The HYDRUS-1D Software Package for Simulating the One-dimensional Movement of Water, Heat, and Multiple Solutes in Variably-saturated Media — Version 3.0,. HYDRUS Software Series 1. 2005. Department of Environmental Sciences, University of California Riverside, Riverside, CA, p. 270.
Soltani, M., Ahmadi, G., 1994. On particle adhesion and removal mechanisms in turbulent flows. J. Adhes. Sci. Technol. 8, 763–785.
Stuart, J.K., Hlady, V., 1995. Effects of discrete protein-surface interactions in scanning force microscopy adhesion force measurements. Langmuir 11, 1368–1374.
Suresh, L., Walz, J.Y., 1996. Effect of surface roughness on the interaction energy between a colloidal sphere and a flat plate. J. Colloid Interface Sci. 183, 199–213.
Tong, M., Johnson, W.P., 2006. Excess colloid retention in porous media as a function of colloid size, fluid velocity, and grain angularity. Environ. Sci. Technol. 40, 7725–7731.
Tong, M., Li, X., Brow, C.N., Johnson, W.P., 2005. Detachment-influenced transport of an adhesion-deficient bacterial strain within water-reactive porous media. Environ. Sci. Technol. 39, 2500–2508.
Torkzaban, S., Bradford, S.A., 2016. Critical role of surface roughness on colloid retention and release in porous media. Water Res. 88, 274–284.
Torkzaban, S., Bradford, S.A., Walker, S.L., 2007. Resolving the coupled effects of hydrodynamics and DLVO forces on colloid attachment in porous media. Langmuir 23, 9652–9660.
Torkzaban, S., Tazehkand, S.S., Walker, S.L., Bradford, S.A., 2008. Transport and fate of bacteria in porous media: Coupled effects of chemical conditions and pore space geometry. Water Resour. Res. 44 n/a-n/a.
Torkzaban, S., Kim, H.N., Simunek, J., Bradford, S.A., 2010. Hysteresis of colloid retention and release in saturated porous media during transients in solution chemistry. Environ. Sci. Technol. 44, 1662–1669.
Torkzaban, S., Bradford, S.A., Wan, J., Tokunaga, T., Masoudih, A., 2013. Release of quantum dot nanoparticles in porous media: role of cation exchange and aging time. Environ. Sci. Technol. 47, 11528–11536.
Tufenkji, N., Elimelech, M., 2004a. Correlation equation for predicting single-collector efficiency in physicochemical filtration in saturated porous media. Environ. Sci. Technol. 38, 529–536.
Tufenkji, N., Elimelech, M., 2004b. Deviation from the classical colloid filtration theory in the presence of repulsive DLVO interactions. Langmuir 20, 10818–10828.
Tufenkji, N., Elimelech, M., 2005. Breakdown of colloid filtration theory: role of the secondary energy minimum and surface charge heterogeneities. Langmuir 21, 841–852.
Vadillo-Rodriguez, V., Busscher, H.J., Norde, W., de Vries, J., van der Mei, H.C., 2004. Atomic force microscopic corroboration of bond aging for adhesion of Streptococcus Thermophilus to solid substrata. J. Colloid Interface Sci. 278, 251–254.
Van Oss, C.J., Chaudhury, M.K., Good, R.J., 1988. Interfacial Lifshitz-van der Waals and polar interactions in macroscopic systems. Chem. Rev. 88, 927–941.
Vandevivere, P., Baveye, P., 1992. Effect of bacterial extracellular polymers on the saturated hydraulic conductivity of sand columns. Appl. Environ. Microbiol. 58, 1690–1698.
Walker, S.L., Redman, J.A., Elimelech, M., 2004. Role of cell surface lipopolysaccharides in *Escherichia coli* K12 adhesion and transport. Langmuir 20, 7736–7746.
Walker, S.L., Hill, J.E., Redman, J.A., Elimelech, M., 2005. Influence of growth phase on adhesion kinetics of *Escherichia coli* D21g. Appl. Environ. Microbiol. 71, 3093–3099.
Wang, Z., Jin, Y., Shen, C., Li, T., Huang, Y., Li, B., 2016. Spontaneous detachment of colloids from primary energy minima by Brownian diffusion. PLoS One 11, e0147368.
Xu, L.-C., Logan, B.E., 2006. Adhesion forces between functionalized latex microspheres and protein-coated surfaces evaluated using colloid probe atomic force microscopy. Colloids Surf. B: Biointerfaces 48, 84–94.
Xu, L.C., Vadillo-Rodriguez, V., Logan, B.E., 2005. Residence time, loading force, pH, and ionic strength affect adhesion forces between colloids and biopolymer-coated surfaces. Langmuir 21, 7491–7500.
Yao, K.-M., Habibian, M.T., O'Melia, C.R., 1971. Water and waste water filtration. Concepts and applications. Environ. Sci. Technol. 5, 1105–1112.
Yee, N., Fein, J.B., Daughney, C.J., 2000. Experimental study of the pH, ionic strength, and reversibility behavior of bacteria-mineral adsorption. Geochim. Cosmochim. Acta 64, 609–617.
Zhang, W., Morales, VnL, Cakmak, M.E., Salvucci, A.E., Geohring, L.D., Hay, A.G., et al., 2010. Colloid transport and retention in unsaturated porous media: effect of colloid input concentration. Environ. Sci. Technol. 44, 4965–4972.